

# Novel Polymer–Ceramic Nanocomposite Based on High Dielectric Constant Epoxy Formula for Embedded Capacitor Application

YANG RAO,<sup>1</sup> S. OGITANI,<sup>2</sup> PAUL KOHL,<sup>3</sup> C. P. WONG<sup>1</sup>

<sup>1</sup> School of Materials Science & Engineering, Package Research Center, Georgia Institute of Technology, Atlanta, Georgia 30332-0245

<sup>2</sup> Asahi Chemical Industry Co. Ltd., 1-3-1 Yako, Kawasaki-Ku, Kanagawa-Ken 210-0863, Japan

<sup>3</sup> School of Chemical Engineering, Package Research Center, Georgia Institute of Technology, Atlanta, Georgia 30332-0100

Received 4 February 2001; accepted 26 May 2001

**ABSTRACT:** Embedded capacitor technology can increase silicon packing efficiency, improve electrical performance, and reduce assembly cost compared with traditional discrete capacitor technology. Developing a suitable material that satisfies electrical, reliability, and processing requirements is one of the major challenges of incorporating capacitors into a printed wiring board (PWB). Polymer–ceramic composites have been of great interest as embedded capacitor material because they combine the processability of polymers with the high dielectric constant of ceramics. A novel nanostructure polymer–ceramic composite with a very high dielectric constant ( $\epsilon_r \sim 110$ , a new record for the highest reported  $\epsilon_r$  value of a nanocomposite) was developed in this work. A high dielectric constant is obtained by increasing the dielectric constant of the epoxy matrix ( $\epsilon_r > 6$ ) and using the combination of lead magnesium niobate–lead titanate (PMN–PT)/BaTiO<sub>3</sub> as the ceramic filler. This nanocomposite has a low curing temperature (<200°C); thus, it is multichip-module laminate (MCM-L) process-compatible. An embedded capacitor prototype with a capacitance density of 50 nF/cm<sup>2</sup> was manufactured using this nanocomposite and spin-coating technology. The effect of the composite microstructure on the effective dielectric constant was studied. This novel nanocomposite can be used for integral capacitors in PWBs. © 2002 John Wiley & Sons, Inc. *J Appl Polym Sci* 83: 1084–1090, 2002

**Key words:** embedded capacitor; polymer-ceramic nanocomposite; metal acacs; SOP

## INTRODUCTION

The microelectronics industry is driven by advances in integrated circuit (IC) technology. As a

result, electronic packaging has advanced in all aspects to meet the interconnection needs of ICs. The evolution of electronic packaging can be categorized into three generations: The first generation of packaging concerned discrete board packaging, which used discrete components that took more than 80% of the board area to support to IC. The second generation used technologies such as chip scale packaging (CSP) and the multichip-

---

Correspondence to: Y. Rao (cp.wong@mse.gatech.edu).  
Contract grant sponsor: Draper Lab.

*Journal of Applied Polymer Science*, Vol. 83, 1084–1090 (2002)  
© 2002 John Wiley & Sons, Inc.  
DOI 10.1002/app.10082

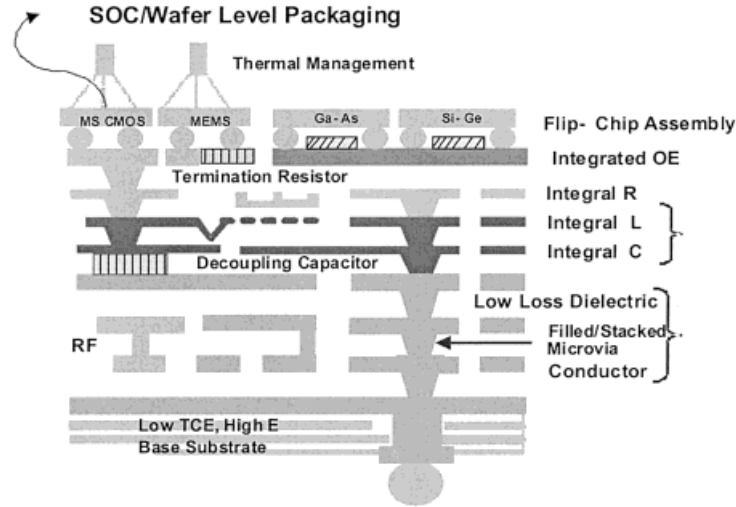


**Figure 1** Schematic view of the single-level integrated module concept.

module (MCM) to increase the silicon packing density to 30–40%. The third generation system on packaging (SOP),<sup>1</sup> proposed by the Packaging Research Center of Georgia Tech, will be based on single-level integrated module (SLIM) technology (as shown in the Fig. 1). SLIM employs a low-cost, large-area organic substrate, on which will be constructed to a multiple level metal-polymer dielectric structure, and provides power, ground, and controlled impedance interconnection functions together with a full range of integral passives and optoelectronics wave-guide structures of the SOP.

Passive devices are electrical elements including resistors, capacitors, and inductors. Passives can be categorized as discrete, integrated, and integral passives, according to the manufacturing process. Figure 2 schematically shows the definition of discrete, integrated, and integral passives.<sup>2</sup> Based on the National Electronic Manufacture Index (NEMI) roadmap, integrated passives are defined as a surface-mounted module formed by many passive components, while integral passives are passive components embedded inside the system board. More than 98% of passives used in the electronic industry are discrete passives. In a typical electronic system, discrete passives outnumber the active ICs by several times and occupy more than 70% real estate of the substrate. Discrete passives have already become the major barrier of the miniaturization of an electronic system. Moreover, integration of passives in packages has the following benefits: better electrical performance, higher reliability, lower cost, and improved design options.

The ratio of capacitors to total passive components can be more than 60%. On the other hand, increasing IC speed requires a decoupling capacitor with a higher capacitance and a shorter distance from its serving components to increase switch performance. Thus, an embedded decoupling capacitor can be a better approach compared with the surface-mounted discrete capacitor. However, embedded capacitors require a very high capacitance density because of the limit in

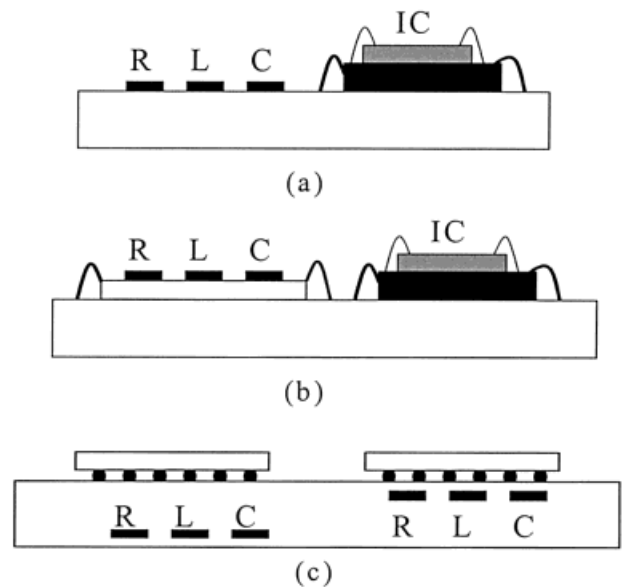


**Figure 2** Various techniques of incorporating passives (R, L, and C) on a substrate: (a) surface-mount discrete passives; (b) integrated passives; (c) integral passives.

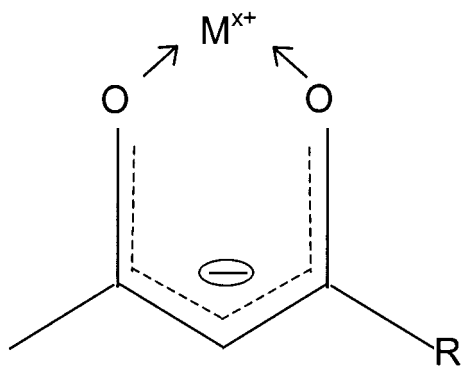


**Figure 3** General structure of metal acac compounds.

their capacitor area. Thus, the insulating material is required to have a very high dielectric constant. One of the biggest constraints of organic-based technology is the low processing temperature required of subsequent layers. Many materials have a high dielectric constant, such as ferroelectric ceramics, but are not suitable for embedded capacitor application, since they require high-temperature processing (e.g., sintering). Polymer–ceramic composites have been studied and are a candidate material for embedded capacitors in organic substrates because they combine the low processing temperature of polymers and the high dielectric constant of ceramics.

Chahal et al.<sup>3,4</sup> obtained an epoxy–ceramic composite with a 70% ceramic volume loading that has a dielectric constant of 74. The traditional approach of a high dielectric constant composite is to increase the ceramic loading of the composite. However, a high ceramic loading (>50 vol %) will dramatically decrease the adhesion of the composite, which will induce process and reliability concerns of embedded capacitors. On the other hand, normal commercial epoxy has a low dielectric constant of around 3–4, which inhibits the effort to increase the effective dielectric constant of the composite at a low ceramic loading level. In this work, the authors studied the effect of metal acetylacetonate (referred to as metal acac) to the dielectric properties of epoxy. The experimental results show that cobalt(III)–acac can dramatically increase the dielectric constant of an epoxy system. Using the modified epoxy, the authors obtained an epoxy–ceramic composite with a higher dielectric constant ( $\epsilon_r = 110$ ) at 70% ceramic volume loading.

An increase in capacitance is attributed to the polarization introduced by the insulator material. There are several molecular mechanisms associ-

ated with this polarization: (a) electronic polarization, (b) atomic polarization, (c) dipole or orientation polarization, and (d) space-charge polarization. *Electronic polarization* is the result of dipole moments induced by the electric field. *Atomic polarization* results from an unsymmetrical sharing of electrons when two different atoms combine to form a molecule. Some molecules have a permanent dipole that can react with an external electric field and form *dipole* or *orientation polarization*. *Space-charge polarization* is different from the previous three types of polarization in that it is not due to charges that are locally bound. Instead, it is produced by charge carriers, such as free ions, that can migrate for some distance throughout the dielectric. The dielectric constant or relative permittivity ( $\epsilon_r$ ) represents the extent of polarization provided by the dielectric material. Most often, the dielectric constant is measured as the ratio of the capacitance of a parallel-plate capacitor with the insulator material compared to the capacitance of the same capacitor with air.<sup>5</sup> The relationship between the capacitance  $C$  and the dielectric constant  $\epsilon_r$  is given by the following equation:

$$C = \frac{\epsilon_0 \epsilon_r A}{t} \quad (1)$$

where  $\epsilon_0$  is the dielectric constant of the free space ( $8.854 \times 10^{-12}$  F/m);  $A$ , the area of the electrical conductor;  $t$ , the thickness of the insulator layer; and  $\epsilon_r$ , the dielectric constant of the insulator layer. Evidently, the larger the dielectric constant, the larger is the capacitance which can be realized in a given space. For this reason, materials with a high dielectric constant are favored in practical design where it is necessary to conserve space.<sup>6</sup>

**Table I** Curing Peak Temperature of Epoxy Formulations

Formulations	Curing Peak Temperature of DER 661	Curing Peak Temperature of ERL 4221
2.5 wt % Co(II)–acac	186°C	197°C
5 wt % Co(II)–acac	184°C	190°C
1.5 wt % Co(III)–acac	190°C	191°C
2.5 wt % Co(III)–acac	186°C	185°C
5 wt % Co(III)–acac	180°C	182°C

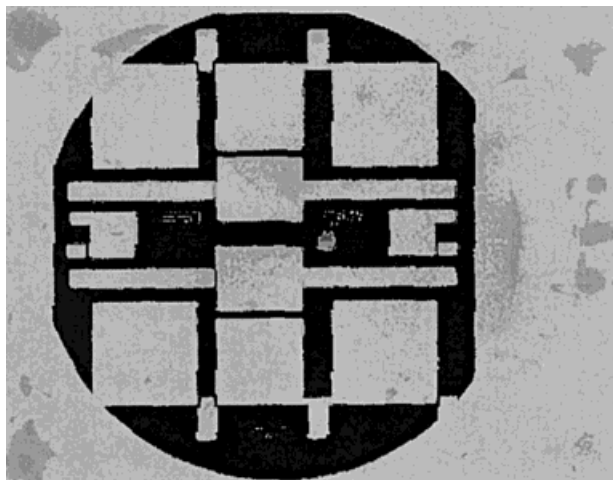


**Figure 4** Prototype of capacitors fabricated by thick-film technology.

## EXPERIMENTAL

Two epoxy resins were chosen as the base polymer: cycloaliphatic epoxy (ERL-4221, from Union Carbide) and bisphenol-A epoxy (DER 661 from Dow Chemical). For ERL-4221, hexahydro-4-methylphthalic anhydride (HMPA, from Aldrich) was chosen as hardener in a 1.0:0.8 mol ratio. This epoxy system has low viscosity, which is helpful for high ceramic loading. The tested dielectric constant of this epoxy system is 3.2 using imidazole (2E4MZ-CN, 1.5 wt %) as a catalyst. DER 661 is in solid form at room temperature and it is dissolved in *N*-methylpyrrolidone (NMP). DER 661 has a reported dielectric constant of 3.7.

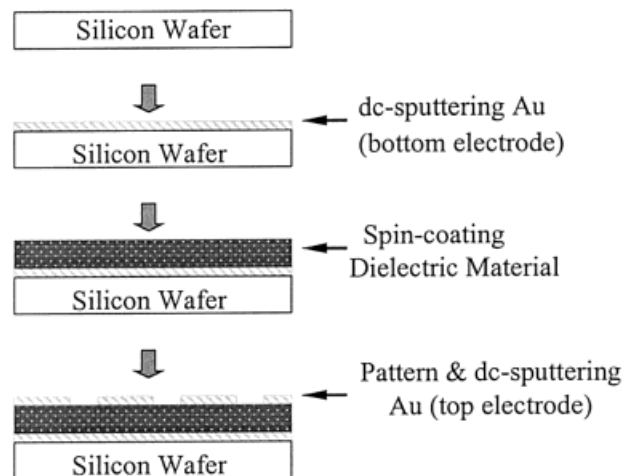


**Figure 5** Fabrication process of prototype of embedded capacitors.

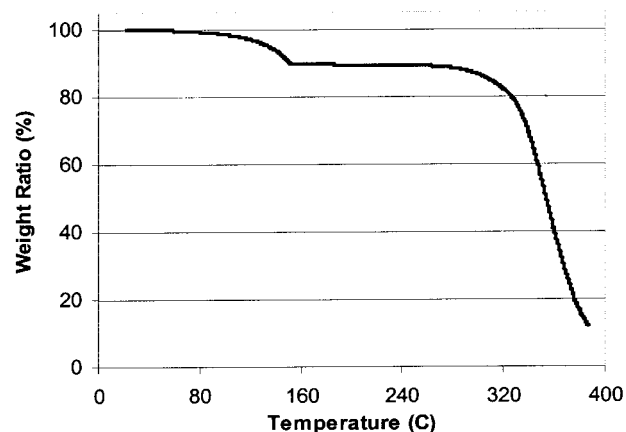


**Figure 6** TGA curve of epoxy system with 5 wt % Co(II)-acac.

To increase the dielectric constant, metal acacs were chosen as additives. Metal acacs possess a  $\beta$ -diketonate structure as shown in Figure 3 and are commonly used as catalysts for epoxy systems.<sup>7</sup> The rationale behind choosing this particular group was that the compound would dissociate during the epoxy curing process, leaving behind metal ions that would increase the polarity of the polymer backbone. The degradation behavior of a series of metal acacs (including transition, lanthanide, actinide, and alkaline earth metals) was studied using thermogravimetric analysis (TGA) (TGA Model 2050, TA Instruments). Cobalt(II)-acac and cobalt(III)-acac were chosen as candidates because they dissociate at a temperature lower than the epoxy system cure temperature (typically  $<200^\circ\text{C}$ ). All these compounds were purchased from Research Organic/Inorganic Chemical and Eastman Kodak.

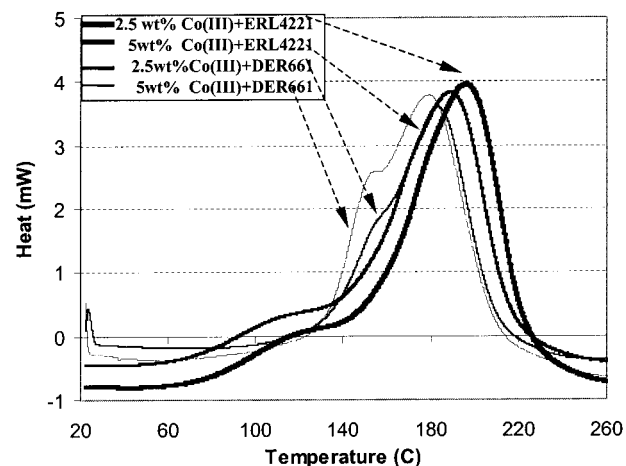


**Figure 7** DSC curves of different epoxy formulations.

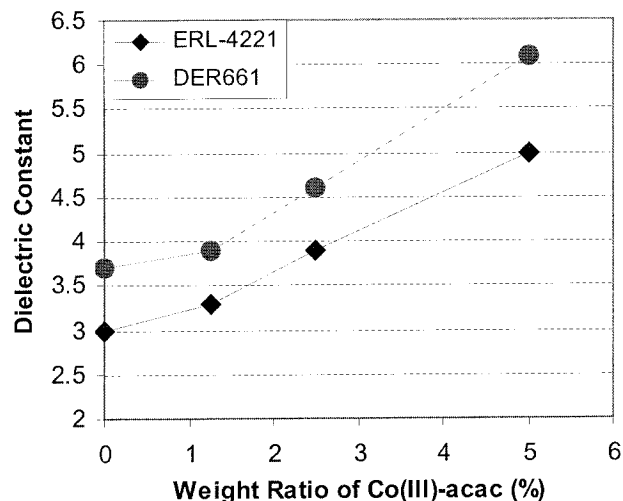
**Table II Dielectric Constant and Loss Factor (Tan  $\delta$ ) from Electrical Testing**

Material	Dielectric Constant	Tan $\delta$
2.5 wt % Co(III) + ERL 4221	3.9	0.017
5.0 wt % Co(III) + ERL 4221	5.0	0.014
2.5 wt % Co(III) + DER 661	4.6	0.015
5.0 wt % Co(III) + DER 661	6.1	0.016
Composite (5 wt % Co(III)–ERL 4221, 70 vol % ceramic)	98	0.017
Composite (5 wt % Co(III)–ERL 4221, 80 vol % ceramic)	89	0.018
Composite (5 wt % Co(III)–DER 661, 70 vol % ceramic)	110	0.016

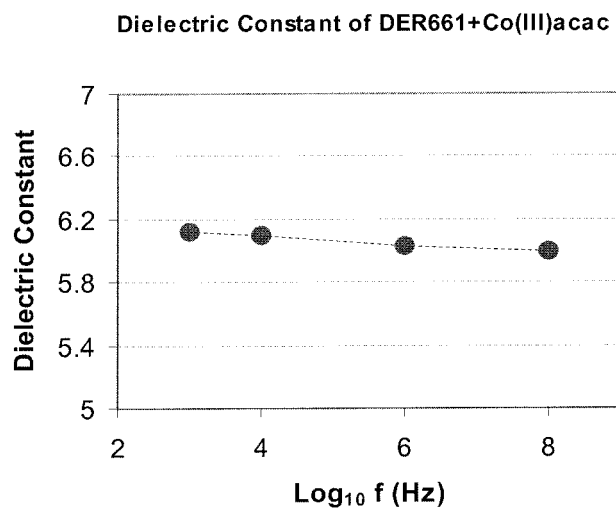
The formulations were made by first dissolving a specific amount of metal acac in warm epoxy resin (70–80°C). Once the additive was completely dissolved, the mixture was cooled to room temperature. Lastly, the hardener was added and the mixture was heated again to 70–80°C while being stirred to achieve a homogeneous blend. Table I gives a list of the epoxy formulations.

To obtain the dielectric constant values for the epoxy system, a prototype of embedded capacitors was fabricated (Fig. 4). Figure 5 shows the fabrication process. At first, a thin layer of gold (0.4  $\mu\text{m}$ ) was deposited on a precleaned and oxidized silicon wafer by dc sputtering. Second, the epoxy was spin-coated onto a gold-coated wafer at 500 rpm for 10 s, then at 2000 rpm for 10 s. The typical thickness of the epoxy layer is around 10  $\mu\text{m}$ . The samples were prebaked at 110°C for 10 min, then cured for 1 h at the temperatures of 30°C lower than the curing peak temperature shown in Table I. This type of curing schedule was used to avoid the appearance of defects and also to ensure full curing of the samples. Next, a thin-film gold (0.2  $\mu\text{m}$ ) pattern was deposited onto the top surface of the film by dc sputtering through a mask. Capacitance measurements were taken using an HP 4263A LCR meter at 1 kHz, 10 kHz, 1 MHz, and 100 MHz. Dielectric constant values were calculated from the capacitance data using eq. (1).

Polymer–ceramic composites were developed using ERL4221 with 5.0 wt % Co(III)–acac and two ceramic fillers: lead magnesium niobate–lead titanate (PMN–PT, from TAM Ceramics) and Ba-

**Figure 8** Dielectric constant of epoxy systems with Co(III)–acac.

TiO<sub>3</sub> (BT-16 from Cabot Inc.). The average particle radius of PMN–PT and BaTiO<sub>3</sub> are 0.9 and 0.065  $\mu\text{m}$ , respectively. The volume ratio of PMN–PT and BaTiO<sub>3</sub> was chosen as 3:1 to obtain a high pack density.<sup>6</sup> Samples containing 70 and 80 vol % filler loading were ball-milled for approximately 4 days at a speed of 220 r/min to obtain a good particle dispersion.<sup>8</sup> The viscosity of the sample was adjusted by the addition of solvents (NMP). The dielectric constant of the composite was also measured using the same method as that for the polymer.

**Figure 9** Dielectric constant of DER661 with 5 wt % Co(III)–acac at different frequencies.

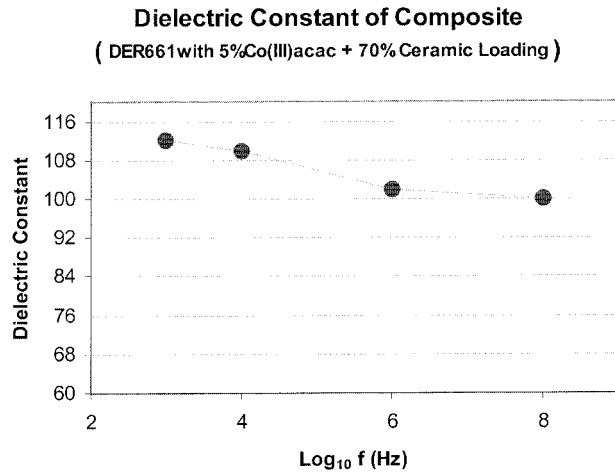


**Figure 10** Dielectric constant of composite at different frequencies.

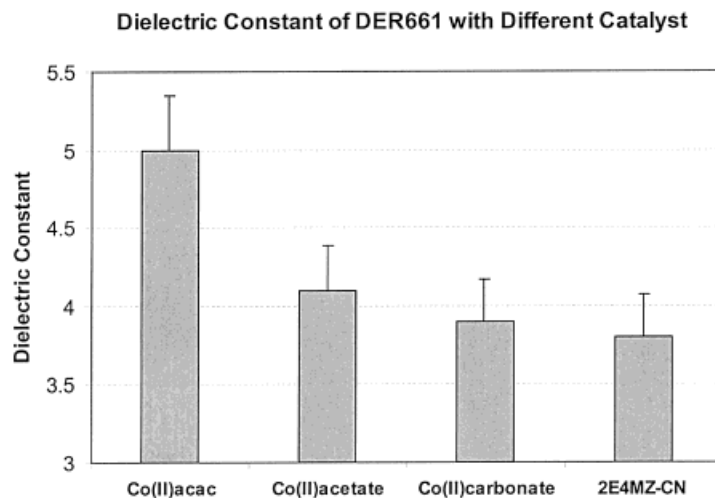
## RESULTS AND DISCUSSION

Figure 6 shows the TGA result of epoxy ERL-4221 with 5 wt % Co(II)-acac. It is obvious that Co(II)-acac dissociates at 150°C. Figure 7 shows the curing profile of four epoxy formulations from differential scanning calorimeter (DSC) analysis.

Table II lists the tested dielectric constants and loss factors of epoxy formulations and composites. Co(III)-acac was found to have a stronger effect on the epoxy system than had Co(II)-acac, although all epoxy formulations with metal acac have a higher dielectric constant. The real mechanism of the dielectric constant increase of epoxy by adding metal acac is still being studied. Figure

8 shows the effect of Co(III)-acac on two epoxy systems.

The dielectric constant of a composite using DER661 with 5 wt % Co(III)-acac and 70 vol % ceramic loading was tested to be 110 (tested at 10 kHz), which is a 50% increase compared with the value of 74,<sup>3</sup> the dielectric constant of the composite using normal epoxy. The dielectric constant of the composite using ERL4221 with 5 wt % Co(II)-I)-acac and 70 vol % ceramic loading was tested to be 98. However, the dielectric constant decreased to 89 for this composite with 80% volume ceramic loading. This may be due to the imperfect dispersing of ceramic particles at a high packing density. Also, it is reported that a high ceramic loading composite may include air in its structure, which could be the reason for the dielectric constant drop. All materials have a low dielectric loss, which is suitable for an embedded capacitor application. Figures 9 and 10 show the dielectric constant change in different testing frequencies for modified DER 661 and the composite, respectively. The dielectric constant decreased less than 10%, from 1 kHz to 100 MHz. The mechanism of the dielectric constant of the epoxy increased by Co-acac was studied. Figure 11 compares the dielectric constant of DER661 with different catalysts: Co(II)acac, CoCO<sub>3</sub>, Co-acetate, and imidazole. It was found that only Co(II)-acac has a strong enough effect to increase the dielectric constant of the epoxy. That may suggest that Co(II)-acac can provide the longer polar side groups that play a crucial role in the polarity increase of the epoxy system.



**Figure 11** Dielectric constant of DER661 with different curing catalysts.

## CONCLUSIONS

Metal acacs were proven to be able to increase the dielectric constant of the selected epoxy systems. Especially, 5 wt % Co(III)-acac can increase the dielectric constant of DER661 about 60%. Using this high dielectric constant epoxy as the matrix, the composite with 70% vol ceramic loading obtained a dielectric constant of 110, which is 50% higher than for a previously reported composite. A prototype of an embedded capacitor with a capacitance density around 50 nF/cm<sup>2</sup> was demonstrated using this novel high dielectric constant composite. The dielectric constant increase of the epoxy by adding Co-acac's may be due to the long polar side group associated with Co-acac's.

The authors gratefully acknowledge Draper Lab. for supporting this work. The authors also would like to thank TAM Ceramics for donating the ceramic materials.

## REFERENCES

1. Tummala, R.; Rymaszewski, E. J.; Klopfenstein, A. G. In *Microelectronics Packaging Handbook*, 2<sup>nd</sup> ed.; Tummala, R., Ed.; International Thompson: New York, 1997.
2. *Passive Components; National Electronic Manufacture Index Roadmap*, 1996 version.
3. Chahal, P.; Tummala, R.; Allen, M. G. In *Proceedings of the International Symposium on Microelectronics*, Orlando, FL, May 28–31, 1996; pp 126–131.
4. Tummala, R. R.; Chahal, P.; Bhattacharya, S. In *IMAPS 35<sup>th</sup> Nordic Conference*, Sweden, Sept. 1998.
5. Grob, B. *Basic Electronics*, 6<sup>th</sup> ed.; McGraw-Hill: New York, 1995.
6. Ogitani, S.; Bidstrup-Allen, S. A.; Kohl, P. In *IPC Conference*, San Diego, CA, April 2–6, 2000.
7. Troutman, T.; Bhattacharya, S.; Tummala, R.; Wong, C. P. In *Proceedings of IMAPS*, Braselton, GA, 1999; p 169.
8. Ogitani, S.; Bidstrup-Allen, S. A.; Kohl, P. In *Proceedings of the 23rd International Electronics Manufacturing Technology Symposium*, 1998; pp 199–205.
9. Liang, S.; Chong, S.; Giannelis, E. In *Proceedings of the 48<sup>th</sup> Electronic Components and Technology Conference*, 1998; pp 171–175.
10. Wong, C. P.; Shi, S. H.; Jefferson, G. *IEEE Trans Compon Pack Manuf Technol A* 1998, 21, 450–458.
11. Rector, J. In *IEEE 48th Electronic Components and Technology Conference*, 1998; p 218.
12. Schaper, L.; Lenihan, T. *Adv Pack* 1998, 22–26.
13. Park, J. Y.; Bhattacharya, S. K.; Allen, M. G. *Fully Integrated Passives Module for Filter Applications Using Low Temperature Process*; ISHM: Philadelphia, PA, 1997; pp 592–597.
14. Das-Gupta, D. K.; Doughty, K. *Thin Solid Films* 1988, 158, 93–105.
15. Mazur, K. In *Ferroelectric Polymers: Chemistry, Physics, and Applications*; Nalwa, H. S., Ed.; Marcel Dekker: New York, 1995.
16. Stauf, G.; Seegel, C.; Watts, R.; O'Bryan, H. In *IMAPS Advanced Technology Workshop on Integrated Passives*, Denver, 1998.
17. Pohl, H. *IEEE Trans Elect Insul* 1986, 683–692.
18. Shrout, T. R.; Hackenberger, W.; Jang, S. J.; Zhang, Q. M.; Randall, C. A. In *IMAPS Advanced Technology Workshop in Integrated Passives*, Denver, 1998.